ARTICLE IN PRESS

Fire Safety Journal ∎ (∎∎∎∎) ∎∎∎–∎∎∎

Contents lists available at SciVerse ScienceDirect

Fire Safety Journal

journal homepage: www.elsevier.com/locate/firesaf

Review

Enabling the study of structure vulnerabilities to ignition from wind driven firebrand showers: A summary of experimental results

Samuel L. Manzello [a,*], Sayaka Suzuki [a], Yoshihiko Hayashi [b]

[a] National Institute of Standards and Technology (NIST), Engineering Laboratory (EL), Fire Research Division, 100 Bureau Drive, Gaithersburg, MD 20899-8662, United States
[b] Department of Fire Engineering, Building Research Institute (BRI), Tachihara 1, Tsukuba, Ibaraki, Japan

ARTICLE INFO

Keywords:
WUI Fires
Firebrands
Ignition

ABSTRACT

The NIST Firebrand Generator (NIST Dragon) is an experimental device that can generate a firebrand shower in a safe and repeatable fashion. BRI maintains one of the only full scale wind tunnel facilities in the world designed specifically for fire experimentation; the Fire Research Wind Tunnel Facility (FRWTF). The coupling of the NIST Firebrand Generator and BRI's FRWTF is leading to progress in assessing vulnerabilities of structures to a firebrand attack. A brief summary of key results to date using the NIST Dragon installed in the FRWTF are provided in this paper as well as a description of the new and improved NIST Dragon's LAIR (Lofting and Ignition Research) facility. The Dragon's LAIR is the only experimental facility capable of simulating continuous wind driven firebrand showers at bench scale. This paper marks the first occasion that all of these findings have been compiled to provide a complete story.

Published by Elsevier Ltd.

Contents

1. Introduction

Structure ignition in the Wildland-Urban Interface (WUI) is a significant international problem with major WUI fires reported in Australia, Greece, Portugal, Spain, and the USA. There have been three significant WUI fires within the past six years in the State of California in the USA. The recent fires in Victoria, Australia in 2009 resulted in over 150 deaths and more than two thousand destroyed structures.

Evidence suggests that wind driven firebrand showers are a major cause of structural ignition in WUI fires in the USA and Australia [1–3]. Japan has been plagued by structural ignition from firebrand showers in urban fires. Building codes and standards are needed to guide construction of new structures in areas known to be prone to these fires in order to reduce the risk of structural ignition in the event of a firebrand attack. Proven, scientifically based retrofitting strategies are required for homes located in areas prone to such fires. To meet these objectives requires knowledge regarding the types of materials that can be ignited by firebrands as well as vulnerable points on a structure where firebrands may easily enter.

* Corresponding author. Tel.: +1 301 975 6891; fax: +1 301 975 4052.
E-mail address: samuelm@nist.gov (S.L. Manzello).

0379-7112/$ - see front matter Published by Elsevier Ltd.
http://dx.doi.org/10.1016/j.firesaf.2012.06.012

For over 40 years, firebrand studies have focused on understanding how far firebrands fly (spotting distance) [4–14]. In a recent comprehensive review article focused on firebrand processes in large fires by Koo *et al.* [15], it is clear that firebrand transport has been the most researched area. Far fewer studies have been performed to understand the firebrand generation process as well as materials that may be vulnerable to ignition from firebrands [15–19]. As a result, prior firebrand research is of limited use to develop ignition resistant structures.

The reason that prior firebrand investigations have not been able to quantify the vulnerabilities of structures to ignition from firebrand showers is that it is difficult to develop a measurement method to replicate wind driven firebrand bombardment on structures that occur in actual WUI and urban fires. Entirely new experimental approaches are required to address this problem. In order to do this, a unique experimental apparatus, known as the NIST Firebrand Generator, has been constructed to generate controlled, repeatable firebrand showers commensurate to those measured from burning conifers and a real WUI fire. Since wind plays a critical role in the spread of WUI fires in the USA and urban fires in Japan, NIST has established collaboration with the Building Research Institute (BRI) in Japan. BRI maintains one of the only full scale wind tunnel facilities in the world designed specifically for fire experimentation; the Fire Research Wind Tunnel Facility (FRWTF).

Two mechanisms are responsible for structural ignition from wind driven firebrand showers: penetration of firebrands inside the structure (such as building vents) and ignition of materials on the exterior of the structure (such as siding treatments or mulch). The coupling of the NIST Firebrand Generator and BRI's FRWTF has enabled the study of both types of vulnerabilities for the first time [20–23].

In this paper, a summary of key results focused on determining these vulnerabilities is delineated. Specifically, results are presented on parametric studies that were focused on exposing roofing assemblies, building vents, siding treatments, walls fitted with eaves, and glazing assemblies to firebrand showers. The danger of firebrand accumulation in front of structures is presented as well. This paper marks the first occasion that all these full scale experiments have been compiled to provide a complete story. This paper is not intended to be a comprehensive review of the entire firebrand literature. Rather it summarizes a new

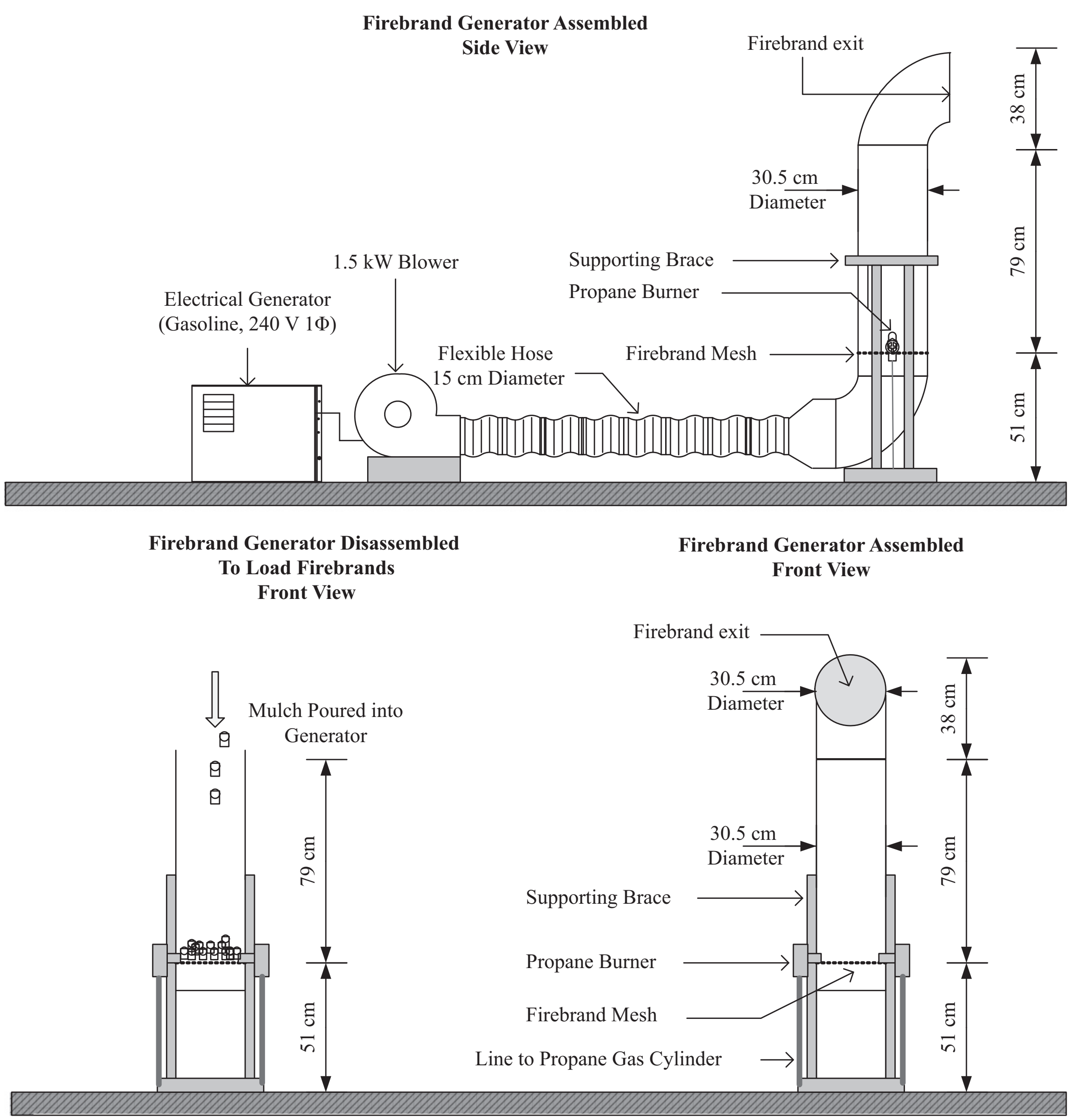

Fig. 1. Schematic of NIST Firebrand Generator (NIST Dragon).

firebrand research area targeted on quantifying structure vulnerabilities to wind driven firebrand showers. This type of firebrand research has not possible prior to the development of the NIST Firebrand Generator described in this paper.

While full scale tests are necessary to highlight vulnerabilities of structures to firebrand showers, reduced scale test methods afford the capability to test new firebrand resistant technologies and may serve as a basis for new standard testing methodologies. Therefore, this paper closes with a brief description of the recently developed NIST Dragon's Lofting and Ignition Research (LAIR) facility. The Dragon's LAIR is the only reduced scale experimental facility capable of simulating continuous wind driven firebrand showers at bench scale.

2. NIST firebrand generator (NIST dragon)

Fig. 1 is a drawing of the NIST Firebrand Generator. A brief description of the device is provided here since a detailed description has been provided elsewhere [20–23]. This version of the device was scaled up from a first-generation, proof-of-concept Firebrand Generator [24]. The bottom panel displays the procedure for loading tree mulch into the apparatus. Tree mulch is used as the fuel source to generate firebrands (details follow below).

The mulch pieces were deposited into the Firebrand Generator by removing the top portion. The mulch pieces were supported using a stainless steel mesh screen (0.35 cm spacing), which was carefully selected. Two different screens were used to filter the mulch pieces prior to loading into the firebrand generator. The first screen blocked all mulch pieces larger than 25 mm in diameter. A second screen was then used to remove all needles from the mulch pieces. The justification for this filtering methodology is provided below. The maximum mulch loading possible with the current Firebrand Generator design is 2.8 kg. The firebrand generator was driven by a 1.5 kW blower.

After the tree mulch was loaded, the top section of the Firebrand Generator was coupled to the main body of the apparatus. The blower was then switched to provide a low flow for ignition. The two propane burners were then ignited individually and simultaneously inserted into the side of the generator. This sequence of events was selected in order to generate a continuous flow of glowing firebrands for up to six minutes duration.

The Firebrand Generator was installed inside the test section of the FRWTF at BRI. Fig. 2 displays a layout of the facility. The facility was equipped with a 4.0 m fan to produce a wind field up to a 10 m/s ($\pm$10%). The wind velocity distribution was verified using a hot wire anemometer array. To track the evolution of the size and mass distribution of firebrands, a series of water pans was placed downstream of the Firebrand Generator. Depending on the structure to be tested, different assemblies were placed downstream of the Firebrand Generator (mock structures, roofing assemblies, etc.).

The Firebrand Generator was designed to produce firebrands characteristic to those produced from burning trees. Prior to designing the Firebrand Generator, Manzello *et. al.* [25,26] conducted a series of experiments quantifying firebrand production from burning trees (see Fig. 3). In that work, an array of pans filled with water was used to collect the firebrands that were generated from the burning trees. The firebrands were subsequently dried and the sizes were measured using calipers and the dry mass was determined using a precision balance. Based on the results of two different tree species of varying crown height and moisture content (Douglas-Fir Trees and Korean Pine Trees) burning singly under no wind, cylindrical firebrands were observed to be

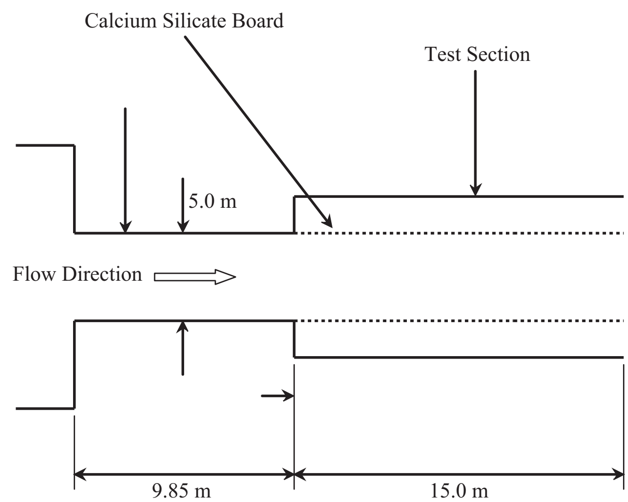

Fig. 2. Schematic of test section of Fire Research Wind Tunnel Facility (FRWTF).

Fig. 3. Photograph of a burning Douglas-Fir tree (5.2 m) used for firebrand collection [25]. This experiment was conducted at NIST's Large Fire Laboratory (LFL).

produced. Douglas-fir was selected as the tree species for the experiments in the USA since it is abundant in the Western United States of America and it is this part of the USA where WUI fires are most prevalent. Korean Pine, another conifer species, was used for comparison to Douglas-Fir. It was observed that more than 85 % of the firebrands produced from these tree experiments were less than 0.4 g [25,26]. Therefore, the filtering procedure for tree mulch used in the Firebrand Generator was selected to produce firebrands with size/mass distributions commensurate to those measured from burning trees (see Fig. 4).

Firebrand size distribution produced using the NIST Dragon is also commensurate with the characteristics of firebrand exposure during a severe WUI fire in California (Angora Fire). The Angora fire burned 1243 ha (3072 ac) and approximately 353 buildings of all types [27]. Digital analyses of burn patterns from materials

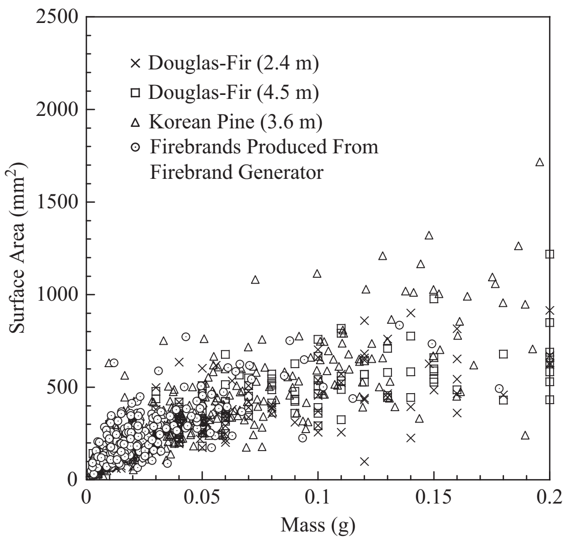

Fig. 4. Firebrands produced from burning trees compared to those produced using the Firebrand Generator. The uncertainty in determining the surface area is ±10%.

Fig. 5. Images of experiments conducted using OSB/CT without bird stops installed [22]. Intense SI was observed within the OSB base layer and eventually FI was observed. The wind tunnel speed was 7 m/s and the Firebrand Generator was located 2.0 m from the CT roofing assembly. The dimensions of the roof assembly were 122 cm by 122 cm.

exposed to the Angora fire were conducted to determine firebrand size distributions. The firebrand size distributions determined from the Angora fire in collaboration with the California Department of Forestry and Fire Protection (CALFIRE), and are believed to be the first of such data from an actual WUI fire. Consistently small sizes of windblown firebrands, similar to those generated using the NIST Dragon, were observed by data collection from the Angora fire. This is in stark contrast with the size of firebrands referenced in existing test standards and wildfire protection building construction recommendations. Further details regarding the quantification of firebrand size distribution are provided elsewhere [27]. The danger of small wind driven firebrand showers is demonstrated in this paper (see below).

The state of combustion of the firebrands generated using the NIST Dragon, namely glowing or flaming, is an important operational parameter that was considered when designing the device. It has been suggested that firebrands fall at or near their terminal settling velocity. As such, when firebrands contact ignitable fuel beds, they are most likely in a state of glowing combustion, not open flaming. It is possible for firebrands to remain in a flaming state under an air flow and, it is reasonable to assume that some firebrands may still be in a state of flaming combustion upon impact. The purpose of the NIST Dragon is to simulate firebrand showers observed in long range spotting and therefore glowing firebrands were desired, yet due to careful design of the NIST Dragon, it is also possible to generate flaming firebrand showers as well. All results presented here are for glowing firebrands.

3. Roofing vulnerabilities

Post-fire studies have long identified a building ignition mechanism in which very small firebrands penetrate under a non-combustible tile roof covering to ignite a building [27]. Although current standards exist (e.g. ASTM E108 [28]) to test ignition of roofing decks to firebrands by placing a burning wood crib on top of a section of a roof assembly under an air flow, the dynamic process of multiple firebrands landing under ceramic tiles/gaps as a function of time is not taken into account. An experimental campaign was conducted to investigate the vulnerabilities of ceramic tile roofing assembles to ignition under a controlled firebrand attack using the NIST Firebrand Generator. A summary of these findings follows; further details regarding these experiments are provided elsewhere [22].

When new, ceramic tile roofing assemblies are constructed by placing a base layer of oriented strand board (OSB), then tar paper (TP) is installed on top of the OSB for moisture protection, and finally ceramic tiles (CT) are applied. Aged or weathered ceramic tile roofing assemblies were simulated by not installing tar paper. For simulated aged ceramic tile roof assemblies, without the installation of bird stops, the firebrands were observed to be blown under the ceramic tiles (see Fig. 5). Bird stops, as the name suggests, are intended to mitigate the construction of nests by birds under the ceramic tiles. During the experiments, eventually, several firebrands would collect and would produce smoldering ignition (SI) within the OSB base layer. With continued application of the airflow, holes were formed within the OSB and eventually the SI would transition to flaming ignition (FI). Simulated aged ceramic tile roof assemblies, with bird stops installed, were also constructed for testing. Even though bird stops were installed, many firebrands were able to penetrate the gaps that exist between the ceramic tiles and the bird stops. These firebrands were observed to produce SI within the OSB base layer; holes were observed in some cases within the OSB base layer. The SI ignition never transitioned to FI when bird stops were applied.

The use of tar paper was then used to simulate a newly constructed ceramic tile roof assembly. With the application of tar paper, experiments were conducted first without bird stops installed. Once again, firebrands were blown under the ceramic tiles. The firebrands were able to burn several holes within the tar paper and produced SI within the OSB base layer. The SI was not intense enough to result in the production of holes within the OSB base layer. Tests were then conducted that considered the application of tar paper with bird stops installed. These conditions resulted in no ignition in the tar paper and thus no ignition within the OSB layer.

The influence of dried pine needles and leaves accumulating under the ceramic tiles was subsequently considered. Even when bird stops were installed, as ceramic tile roof assemblies were exposed to the elements over time, the deposition of dead needles and leaves under the tiles would be expected. The result, summarized above, namely that the combination of the bird stop installation

Please cite this article as: S.L. Manzello, et al., Enabling the study of structure vulnerabilities to ignition from wind driven firebrand showers: A summary of experimental results, Fire Safety J (2012), http://dx.doi.org/10.1016/j.firesaf.2012.06.012

coupled with the tar paper application provided a barrier to ignition, does not hold true if dead needles and leaves were placed under the tiles. If needles and leaves are deposited under the tiles, ceramic tile roofing assemblies are ignitable under all conditions considered in this study.

All of the experiments summarized above considered perfectly aligned roofing tiles that would be expected in new roof construction. As ceramic tile roof assemblies age, the tile alignment does not remain so closely spaced. In fact, large gaps develop within the tiles themselves leading to openings where firebrands may enter and accumulate. To quantify this vulnerability, a final series of experiments were conducted where the ceramic tiles were not fit together perfectly. The types of gaps simulated were based on surveys of actual roofs. Due to the presence of gaps within the tiles, ignition under the tiles within the OSB base layer was observed: (1) whether or not bird stops were installed, (2) whether or not tar paper was installed. This result is somewhat obvious and suggests that when gaps exist within the alignment of the ceramic tiles, ignition of the assembly is rather easy. The application of dead needles and leaves was not even considered with gaps present in the ceramic tiles as this would only compound the vulnerabilities to ignition. These results are the first ever experiments to ascertain the vulnerabilities of ceramic tile roofing assemblies.

In addition to investigating ceramic tile roofing assemblies, full scale sections of asphalt shingle roofing assemblies were constructed and exposed to firebrand showers; a summary of these results follows with more details available in Manzello *et al.* [21]. Both flat roof sections as well as angled (valleys) were considered. The full scale sections constructed for testing included asphalt shingle roofing assemblies (OSB, tar paper, and asphalt shingles) as well as only base layer roofing materials, such as OSB. It is important to realize that bare OSB is not used as the surface material in roofing but roofs in a state of ill repair may easily have base layer materials such as OSB exposed to firebrand showers.

For ignition testing of roofing base layer materials (OSB), at an angle of 60°, the firebrands were observed to collect inside the channel of the OSB crevice (see Fig. 6a–c). The firebrands that collected in the crevice produced SI where they landed, eventually resulting in several holes in the OSB. The OSB continued to smolder intensely near the locations where the firebrands landed. Eventually a transition to FI was observed on the back side of the OSB. As the angle was increased to 90°, similar behavior was observed where the firebrands that collected initiated intense smoldering. Eventually, holes were formed at these locations in an identical manner to the 60°. While SI was observed, it was not possible for a transition to flaming to occur. As the angle was increased to 135°, ignition was no longer possible.

With regard to ignition testing of roofing valleys (OSB, tar paper, and asphalt shingles), at 60° and 90°, several firebrands were observed to become trapped along the channel of two sections and along the seams of the shingles. However, no ignition events were observed. The firebrands were only capable of melting the asphalt shingles (see Fig. 7). As the angle was spread further, fewer firebrands were observed to become trapped in the seam of the two sections, in a similar manner to the base layer OSB tests. While these tests did not consider the influence of aged

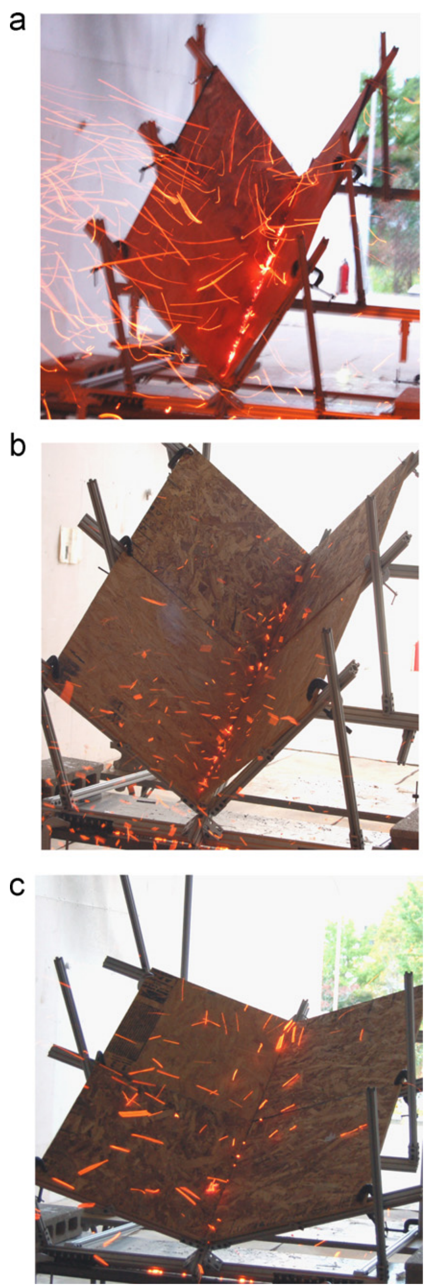

Fig. 6. Bare OSB full scale sections used for testing [21]. (a) Angle of 60°; smoldering ignition observed, (b) angle of 90°; smoldering ignition observed and (c) angle of 135°; no ignition observed. The wind tunnel speed was 7 m/s in each case and the overall dimensions of the OSB sections were 122 cm by 122 cm.

Fig. 7. Fig. 6 OSB base layer, tar paper, and asphalt shingles; angle of 90°-no ignition observed [21]. The wind tunnel speed was 7 m/s. The dimensions of the assembly were 122 cm by 122 cm.

Please cite this article as: S.L. Manzello, et al., Enabling the study of structure vulnerabilities to ignition from wind driven firebrand showers: A summary of experimental results, Fire Safety J (2012), http://dx.doi.org/10.1016/j.firesaf.2012.06.012

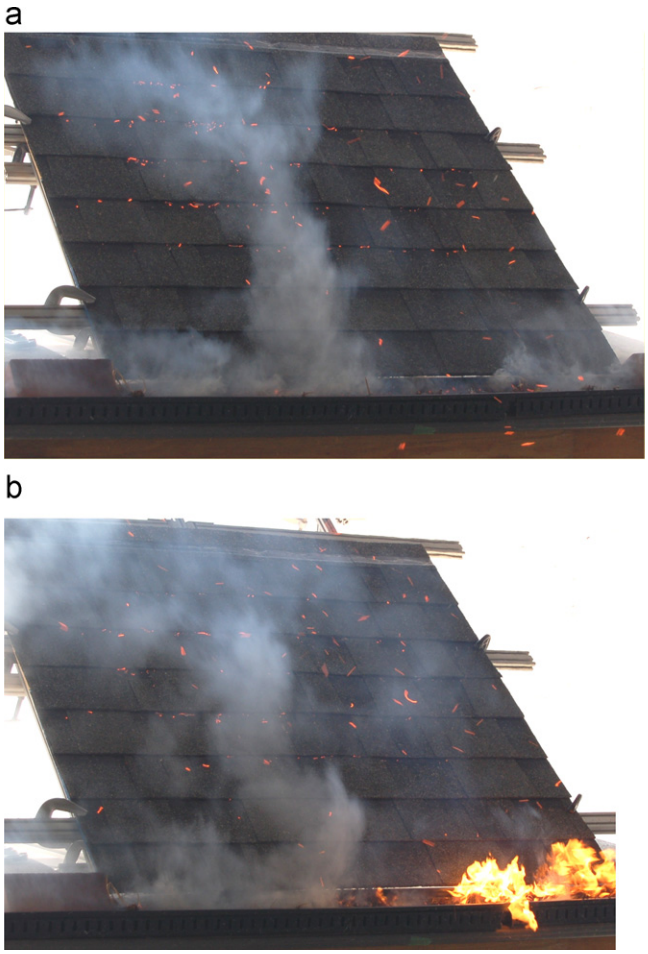

Fig. 8. Section of full scale roof assembly [21]. (a) Smoldering ignition of needles/leaves inside gutter and (b) transition to flaming ignition. The wind tunnel speed was 7 m/s and the roof assembly had dimensions of 122 cm by 122 cm.

or pre-heated shingles, the results clearly indicate that firebrands can melt asphalt shingles.

Pine needles in the gutters of homes may be susceptible to ignition by firebrand showers. To investigate this, a flat roof section was built and a gutter was attached to the front. The gutter was constructed of polyvinyl chloride (PVC); a gutter material found in new home construction. As in the roof valley experiments described above, OSB was used as the base layer; tar paper and shingles were then applied. Dried pine needles and leaves were used and placed inside the gutter.

Fig. 8a, b displays typical results obtained from the experiments. The firebrands that were deposited inside the gutter produced SI inside the gutter. The smoldering intensified and ultimately this transitioned to FI. The asphalt shingles were observed to melt once exposed to the intense flaming that occurred inside the gutter. The flames, however, did not spread up the roof section. While the flames did not spread upwards along the roof, these images are very important since they clearly show the dangers of not cleaning gutters. The influence of pre-heated shingles as well as aged shingles was not addressed.

4. Building vent vulnerabilities

The 2007 California Building Code of Regulations, Title 24, Part 2, Chapter 7A, desired to mitigate firebrand penetration through building vents by recommending a metal mesh of 6 mm be placed behind building vents [29]. Yet, this mesh size was not based on any scientific testing since no test methods were available at that time. Therefore, the Firebrand Generator was used to study the penetration of firebrands into building vents [20]. In that work, firebrand penetration into a gable vent fitted with a mesh assembly (only three mesh sizes were used—6.0 mm, 3.0 mm, and 1.5 mm opening) was investigated and shredded paper was placed behind the mesh to determine if firebrands that penetrated the vent and subsequent mesh were able to produce an ignition event [20]. That study showed that firebrands were not quenched by the presence of the mesh and would continue to burn on the mesh until they were small enough to pass through the mesh opening. For the 6 mm mesh, a majority of the firebrands simply flew through the mesh, resulting in more rapid ignition of flammable materials behind the mesh than that observed for the smaller mesh sizes of 3 mm and 1.5 mm.

Recently, a more in depth investigation aimed at extensively quantifying firebrand penetration through building vents using full scale tests at BRI was completed in collaboration with ASTM (details below). Namely, six different mesh sizes were considered, from 5.72 mm to 1.04 mm opening, as well as four different types of ignitable materials placed inside the structure. This greater range of parameters allowed for the generation of a database of firebrand penetration behavior and subsequent ignition of materials placed behind varying mesh sizes. A summary of these findings is provided elsewhere [23].

The overall dimensions of the target structure, placed 7.5 m downstream of the NIST Dragon, were 3.06 m in height, 3.04 m in width, and 3.05 m in depth. The structure was constructed of calcium silicate (non-combustible) board. A generic building vent design, consisting of only a frame fitted with a metal mesh, was used. The vent opening was fitted with six different types of metal mesh: 4×4 mesh $\times0.65$ mm wire diameter, 8×8 mesh $\times0.43$ mm wire diameter, 10×10 mesh $\times0.51$ mm wire diameter, 14×14 mesh $\times0.23$ mm wire diameter, 16×16 mesh $\times0.23$ mm wire diameter, and 20×20 mesh $\times0.23$ mm wire diameter. These mesh sizes corresponded to opening sizes of: 5.72 mm (4×4), 2.74 mm (8×8), 2.0 mm (10×10), 1.55 mm (14×14), 1.35 mm (16×16), and 1.04 mm (20×20). Mesh was defined, per the manufacturer, as the number of openings per 25.4 mm (1'').

Behind the mesh, four different materials (all materials were oven dried) were placed to ascertain whether the firebrands that were able to penetrate the building mesh assembly could ignite these materials. The materials were shredded paper, cotton, crevices constructed with OSB and wood (to form 90° angle). For the crevice tests, experiments were conducted with the crevice filled with or without shredded paper. The purpose of using the crevice was to determine if firebrands that penetrated the mesh were able to ignite building materials. Paper in the crevice was intended to simulate fine fuel debris.

For the full scale tests, the wind tunnel speed was fixed at 7 m/s. The velocity behind the mesh varied from 7 m/s (4×4 mesh; 5.72 mm opening) to 5 m/s (20×20 mesh; 1.04 mm opening).

Three repeat experiments were conducted for each of the four ignitable materials considered and the results are tabulated in Table 1. When shredded paper was used, a repeatable SI was observed for all mesh sizes up to 16×16 (1.35 mm). As for the smallest mesh size tested (20×20) (1.04 mm), SI was observed in only one experiment out of three. For cotton, the ignition behavior was similar for all mesh sizes. The firebrands would deposit into the cotton bed and simply burn holes into the cotton.

The bare wood crevice experiments resulted in SI in the OSB layer for the 4×4 (5.72 mm) and 8×8 (2.74 mm) mesh sizes. As the mesh size was reduced to 10×10 (2.0 mm), the firebrands were not able to ignite the bare wood crevices. When the crevices

Please cite this article as: S.L. Manzello, et al., Enabling the study of structure vulnerabilities to ignition from wind driven firebrand showers: A summary of experimental results, Fire Safety J (2012), http://dx.doi.org/10.1016/j.firesaf.2012.06.012

Table 1
Summary of full scale tests at BRI. 72 experiments were conducted.

Mesh	Paper	Cotton	Crevice	Crevice with paper
4 × 4 (5.72 mm)	SI to FI	SI	SI	SI to FI (paper) SI (OSB)
8 × 8 (2.74 mm)	SI to FI	SI	SI	SI to FI (paper) SI (OSB)
10 × 10 (2.0 mm)	SI to FI	SI	NI	SI to FI (paper) (SI OSB)
14 × 14 (1.55 mm)	SI	SI	NI	SI (paper) SI (OSB)
16 × 16 (1.35 mm)	SI	SI	NI	NI
20 × 20 (1.04 mm)	Two tests: NI; One test SI	Two tests: SI; One Test NI	NI	NI

NI—no ignition; *SI*—smoldering ignition; *FI*—flaming ignition.

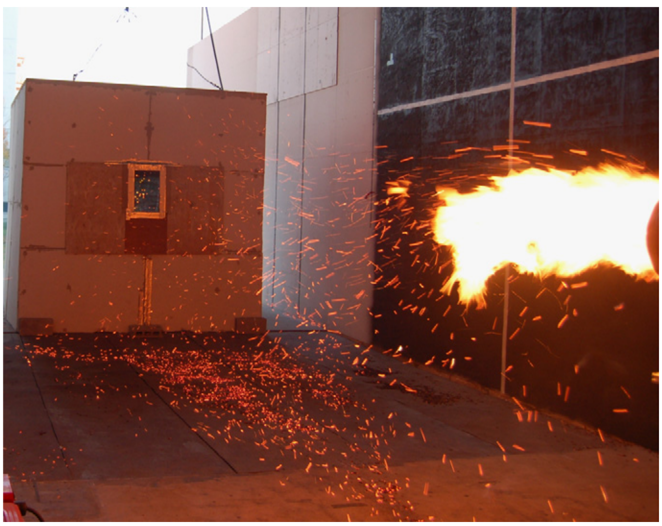

Fig. 9. Typical experiment using NIST Firebrand Generator at BRI's FRWTF [23]. The mesh installed in this experiment was 20 × 20 (1.04 mm), the wind tunnel speed was 7 m/s, and the Firebrand Generator was located 7.5 m from the structure. The dimensions of the structure were 3.06 m in height, 3.04 m in width, and 3.05 m in depth and it was constructed of calcium silicate (non-combustible) board.

were filled with shredded paper, SI followed by FI occurred in the paper for mesh sizes up 10 × 10 (2.0 mm). The OSB layer was then observed to ignite by SI and subsequently produced a self sustaining SI that continued to burn holes into the OSB. For the smallest mesh sizes tested (16 × 16 and 20 × 20), NI was observed in the paper and consequently NI in the crevice. A photograph of a typical experiment is shown in Fig. 9.

In summary, these experiments found that firebrands were not quenched by the presence of the mesh and would continue to burn until they were able to fit through the mesh opening, even down to a 1.04 mm opening (shown in Fig. 10). Mesh size reduction did mitigate ignition of bare wood crevices. Yet, ignition of fine fuel was still observed as mesh size was reduced suggesting that firebrand resistant vent technologies would be helpful.

During the 2010 triennial code change cycle in California, no standard test methods were available to evaluate and compare firebrand resistant vent technologies. Therefore, NIST worked with the California Department of Forestry and Fire Protection (CALFIRE) as part of a task force in order to reduce mesh size used to cover building vent openings to lessen the potential hazard of firebrand entry into structures. These changes were formally adopted into the 2010 California Code of Regulations, Title 24, Part 2, Chapter 7A, and are effective from January 2011, onward [30].

An ASTM task group on vents, organized within Subcommittee E05.14.06, External Fire Exposures, has been working to develop a reduced scale test method (not presently a standard) aimed at evaluating the ability of vents to resist firebrand intrusion into attic and crawl space areas. In this test method, firebrands are produced by igniting wood pieces and the firebrands are subsequently deposited on top of the vent installed in the test chamber. The vent is placed horizontally in the apparatus and air is pulled through the vent using a fan placed downstream. The mechanism of firebrands residing on top of vents and being pulled down onto vents is not representative of the actual situation. Firebrands are actually blown onto the vents themselves.

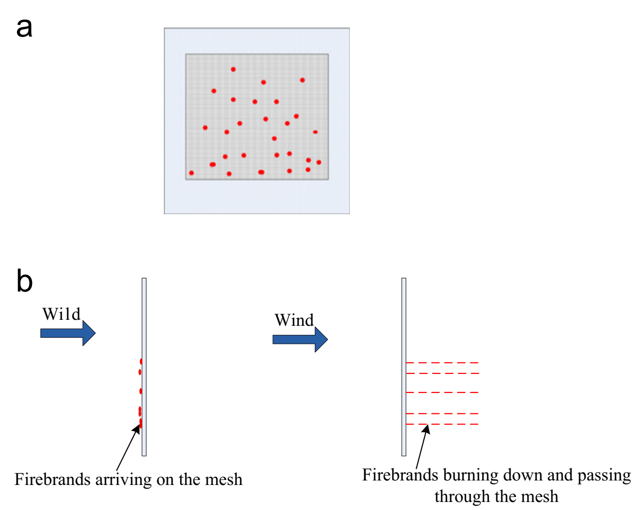

Fig. 10. Schematic of firebrand penetration through a mesh. The identical behavior was observed in both full scale and bench scale experiments. (a) Front view and (b) side view.

Therefore, a comparison testing protocol was undertaken, with the formal support [31] of the ASTM E05.14.06 task group, between the method developed by ASTM to the full scale experiments using the NIST Firebrand Generator at BRI's FRWTF as these full scale tests developed by BRI/NIST attempt to simulate a wind driven firebrand attack that is seen in actual WUI fires. This comparison testing protocol was undertaken to determine if the reduced scale method (ASTM) was able to effectively represent firebrand penetration through building vents observed using the full scale test method. The results of the comparison testing protocol are beyond the scope of this paper, are the subject of a future publication, and have been balloted as part of an ASTM standard.

5. Siding treatment vulnerabilities

Anecdotal evidence exists related to vulnerabilities of siding treatments, walls fitted with eaves, and glazing assemblies to firebrand attack, yet standard test methods are not available to evaluate the ability of these construction elements to resist firebrand showers. Before the development of the NIST Firebrand Generator and the subsequent coupling of this device to the FRWTF, there was no method to actually generate firebrand

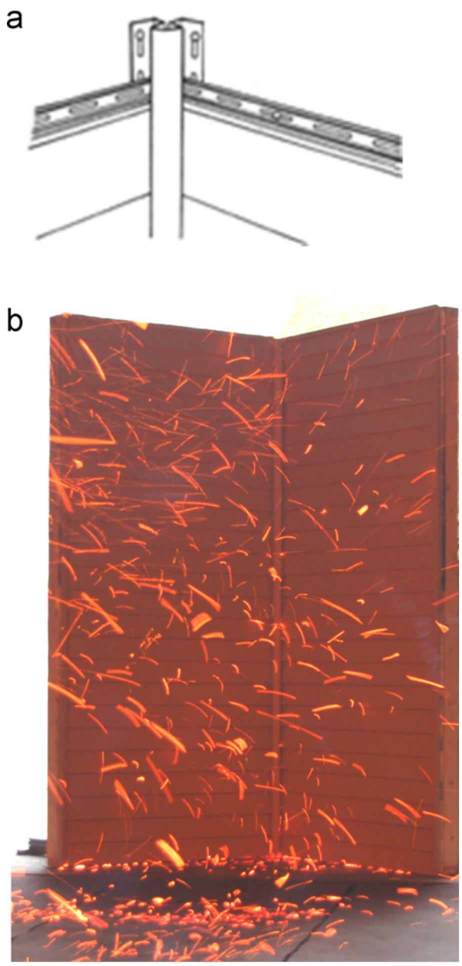

Fig. 11. (a) Drawing of a corner post and (b) picture of vinyl siding reentrant corner assembly under firebrand bombardment [33]. The dimensions of each side of this assembly were 122 cm wide by 244 cm high.

showers in a controlled, laboratory setting to quantify these vulnerabilities. Therefore, a workshop was held in June, 2010, by NIST to provide input on the type of siding treatments, eaves assemblies, and glazing assemblies most common and important to consider for experimentation [32]. The focus has been placed on the state of California since many large WUI fires have occurred there over the past 10 years [32].

Siding treatments applied in a reentrant corner configuration are believed to be the most vulnerable to firebrand showers, since firebrands may become trapped not only under the siding itself but also within the corner post (see Fig. 11a; corner posts commonly used for vinyl and polypropylene siding). For cedar shingle siding, it is also believed that wind driven firebrands may ignite the siding material itself.

Therefore, a parametric study was performed in an effort to quantify the range of conditions that siding treatments are vulnerable to ignition from firebrand showers. Three different siding treatments were used: vinyl siding, polypropylene siding, and cedar shingle siding (untreated and fire retardant treated). Detailed results for the vinyl and polypropylene siding were described in a recent journal publication [33]; the cedar shingle siding results are presented in the archival literature for the first time.

A full scale reentrant corner section (each side was 122 cm wide by 244 cm high) assembly was constructed for testing. To be able to control the moisture content of the OSB sheathing, the experiments were designed in a modular fashion. Specifically, each side of the 122 cm by 244 cm full section was comprised of 12 separate OSB pieces. This allowed each section to be oven dried and simply reassembled inside the custom mounting frame. For each assembly, a moisture barrier was applied (Tyvek,[1] a registered product of DuPont, was used for the vinyl and polypropylene siding; felt underlayment was used for the cedar siding) and then the siding treatments were applied. The frame was constructed using wood studs with a stud spacing of 406 mm (16") on center. The American Vinyl Siding Institute and the Cedar Shake and Shingle Bureau (wall manual) were consulted for proper installation and construction was performed in accordance with their respective installation manuals [34,35].

Similar to the roofing and vent studies, a starting velocity of 7 m/s was selected since most of the firebrands produced from the Firebrand Generator were observed to be lofted under these conditions. The velocity was subsequently increased to 9 m/s to ascertain if any the results were velocity dependent. Three replicate experiments were conducted for each wind speed.

For experiments with vinyl siding (see Fig. 11b for typical experiment) conducted at 7 m/s and 9 m/s, the firebrands were observed to melt the siding to the point where holes developed through the material. A picture of this is shown in Fig. 12. While burns were observed in the moisture barrier at both wind speeds (Tyvek), ignition of the OSB sheathing was only observed for vinyl siding tests at 9 m/s and when the sheathing was dried. It is important to point out that the OSB sheathing burned completely through and ignition was observed within the wood framing members as well (2×4).

For polypropylene siding, firebrands produced melting within the material but no holes were formed within the siding itself. Firebrands were observed to penetrate the corner post and burn holes into the moisture barrier (Tyvek) but ignition was never observed in the OSB sheathing for any wind speed of moisture content considered. Nevertheless, it is important to point out that firebrands easily penetrated the corner post in both siding types.

Experiments were conducted for untreated cedar shingle siding. Since it was not possible to dry the cedar shingle siding under full scale experimental conditions, experiments were conducted by exposing the same reentrant corner assembly to repeat exposures using the NIST Dragon. The moisture content of the cedar shingle siding at the time of testing was determined to be 11% on a dry basis (see Eq. (1); M_{wet} and M_{dry} correspond to the weight and dry mass) and the wind tunnel speed was 7 m/s.

$$Moisture\ Content = \frac{M_{wet} - M_{dry}}{M_{dry}} \times 100, \quad (1)$$

The exposure time of firebrands from the NIST Dragon is six minutes and it is possible to load the device and start a new experiment within ten minutes of completing the prior test; therefore three exposure tests can be conducted relatively quickly. After the first exposure, essentially nothing was observed to happen since the moisture of the cedar was too high to produce smoldering ignition. It was observed that after the third exposure to firebrand showers, the cedar shingle siding ignited at the base of the wall assembly. These results qualitatively demonstrate that continual firebrand bombardment may produce smoldering ignition of moist cedar, even under full scale applications.

Finally, the vulnerability of fire retardant cedar shingles was investigated. The 2010 California Code of Regulations, Title 24, Part 2, Chapter 7A, that are effective from January 2011, onward allows fire-retardant-treated wood shingles listed for use as

[1] The identification of any commercial product or trade names does not imply endorsement or recommendation by NIST.

Fig. 12. Image of vinyl siding (from bottom) after firebrand exposure at 7 m/s [33].

Fig. 13. In the top image, firebrands have caused smoldering ignition in the mulch bed [33]. In the bottom image, smoldering ignition has transitioned to flaming ignition and the wall assembly has ignited. The dimensions of the wall assembly were 244 cm by 244 cm.

"Class B" roof covering (evaluated based on ASTM E108 [28]) as acceptable as an ignition-resistant wall covering material when installed over solid sheathing [30]. To the authors' knowledge, this new addition to the code was not based on scientific testing.

Fig. 14. Images of untreated cedar shingle siding ignited under firebrand attack at a wind tunnel speed of 7 m/s. The dimensions of each side of this assembly were 122 cm wide by 244 cm high.

As a result, this type of fire retardant cedar shingle siding was exposed firebrand showers. After repeated exposures to wind driven firebrand showers, no ignition of the cedar shingle siding material was observed.

Experiments were also conducted to determine if firebrands can produce ignition in fine fuels placed adjacent to the wall assembly and whether the subsequent ignition of fine fuels could lead to ignition of the wall assembly itself. In these experiments, vertical walls in addition to reentrant corners were used. Dead tree needles were placed adjacent to the wall assembly to simulate fine fuels likely to be placed near a structure (such as pine straw mulch). The basis for using pine needles was predicated on the fire hazard expected from this fuel source observed in reduced scale experiments. In prior work, using reduced scale experiments, Manzello et al. [36] demonstrated that glowing firebrands are capable of producing smoldering igniting of pine needle beds and under an applied air flow, SI of pine needle beds was observed to transition to FI.

Firebrands were observed to ignite the needle bed via SI, the smoldering ignition become self-sustaining, and a transition to FI was observed (see Fig. 13). The FI in the needles subsequently melted the vinyl siding and produced self-sustaining SI at the base of the wall assembly (within the OSB; this OSB was not even dried).

When considering untreated cedar shingle siding, similar results were observed; namely ignition of wall assembly itself (see Fig. 14). The fire retarded cedar shingle siding performed very well. Even though the fine fuels exposed the wall assembly to flames, ignition of the cedar shingle siding was not observed, nor did any ignition occur in the OSB sheathing.

6. Eave vulnerabilities

An interesting question is whether firebrands may become lodged within joints between walls and the eave overhang. There are essentially two types of eave construction commonly used in California and the USA [37]. In open eave construction, the roof rafter tails extend beyond the exterior wall and are readily visible. In the second type of eave construction, known as boxed in eave construction, the eaves are essentially enclosed and the rafter tails are no longer exposed. Since the open eave configuration is believed to be the most vulnerable to firebrand showers, some jurisdictions prone to intense WUI fires have required eaves be boxed in. In both construction types, vents may be installed [37].

Consequently, the open eave construction, thought to be the most vulnerable configuration situation, was used for experimentation. An eave with a total length of 122 cm overhang was constructed and mounted to a 2.44 m by 2.44 m wall assembly. While the eave was 122 cm long, the actual overhang used was 61 cm. Since the purpose of these experiments was to determine if any accumulation of firebrands was observed within the eave assembly, the wall was simply fitted with OSB sheathing and it was not dried. The wall was constructed using wood framing members spaced 406 mm (16'') on center. Details of these results were presented in a recent journal publication [33].

In half of the experiments, no vent opening was used to simply observe if firebrands actually accumulated within the exposed rafters and subsequent joints (see Fig. 12). In the remaining experiments, vents were installed (see bottom panel) and a mesh was placed within the vent opening (see Fig. 15). For the vent openings, 50 mm holes were drilled into the blocking material and an 8×8 mesh (2.75 mm opening) was secured, as recommended in the new, 2010 California WUI code [30]. Three

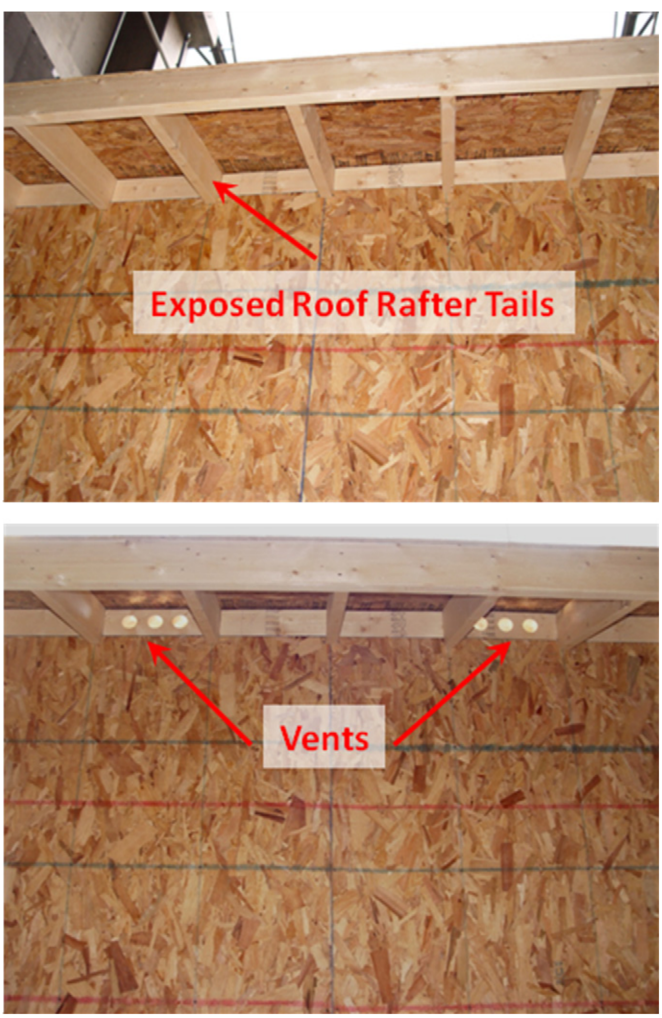

Fig. 15. Images of open eave construction with no vents (top) and vents (bottom) [33]. In both images, the wall dimensions were 244 cm by 244 cm. The eave overhang was 61 cm.

Fig. 16. Image of wall fitted with eave under firebrand bombardment [33]. The wall dimensions were 244 cm by 244 cm with a 61 cm eave overhang.

replicate experiments were performed. For the experiments that used no vent opening, firebrands were not observed to accumulate under the eave over the range of wind speeds considered (see Fig. 16 for a typical experiment).

The NIST Fire Dynamics Simulator (FDS) was used to visualize the flow around the eave assembly in the FRWTF in an attempt to gain insight as to reasons why accumulation of firebrands were not observed under the eave assemblies for wind speeds of 7 m/s and 9 m/s [33]. FDS is a computational fluid dynamics model of fire-driven fluid flow and numerically solves a form of the Navier-Stokes equations appropriate for low-speed, thermally driven flow. While FDS was designed with fire in mind, it may be used, as in the case of the simulations conducted in this study, for low-speed fluid flow simulations that do not involve fire [38]. The results of the simulations are presented in Fig. 17. The dimensions of the eave assembly are identical to those used in the actual experiments and numerical grid spacing was 5 cm. As mentioned, the flow profile inside the FRWTF was mapped using a series of hot wire anemometers (21 point array). Based on these measurements, the flow profile was observed to be uniform. As a result, in these simulations, the flow profile inside FRWTF was assumed uniform and fixed at 9 m/s.

Although firebrands are not modeled, the resulting air flow profiles demonstrate why accumulation of firebrands was difficult under the eave (see Fig. 17). Specifically, the presence of the wall results in a large stagnation zone in front of the wall that becomes

Please cite this article as: S.L. Manzello, et al., Enabling the study of structure vulnerabilities to ignition from wind driven firebrand showers: A summary of experimental results, Fire Safety J (2012), http://dx.doi.org/10.1016/j.firesaf.2012.06.012

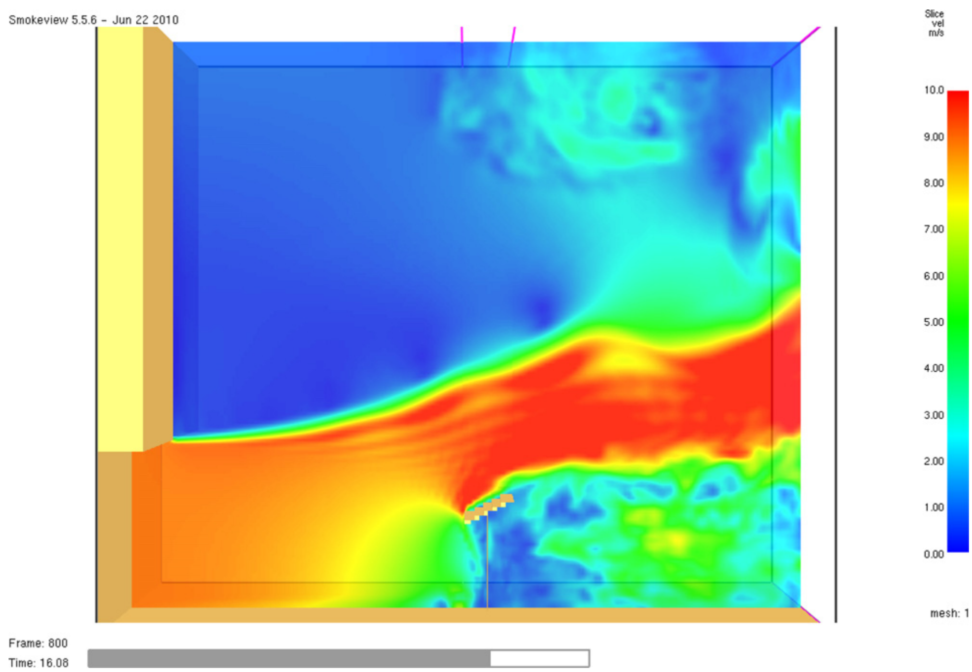

Fig. 17. FDS simulations of air flow around eave assemblies for a wind speed of 9 m/s [33]. The dimensions of the eave assembly are identical to those used in the actual experiments (see Fig. 16) and numerical grid spacing was 5 cm.

more pronounced as wind speed was increased. In addition, under the eave there is an area of little or no flow velocity that would be required to drive the firebrands into the joints between the eave and wall assembly. It is important to point out that these simulations considered only airflow and do not include the seeding of firebrands into the flow. Current work at NIST is aimed at incorporating a firebrand transport model into the newly developed Wildland-Urban Interface (WUI) Fire Dynamics Simulator (WFDS).

When vents were installed, cameras were placed both in front and behind of the eave assembly in order to quantify the number of firebrands arriving at the vent locations. At 7 m/s, the number of firebrands arriving at the vent location was 10 ± 1 (average $\pm$ standard deviation). As the velocity was increased to 9 m/s, the total number of firebrands arriving at the vent location increased to 28 ± 2 (average $\pm$ standard deviation). While the number of firebrands arriving at the vent locations increased as the wind speed increased, it was very small as compared to the number of firebrands that bombarded the wall/eave assembly.

Firebrand entry into vents has long been thought to be important. Based on input garnered from the NIST workshop in California [32], for the present experiments using vents, it was desired to construct the wall from a combustible material to determine whether the wall itself could be ignited by firebrands within the time of the firebrand exposure (six minutes). Prior work by Manzello *et al.* [20,23] used non-combustible construction to investigate only vent penetration and ignition of materials inside the structure. During the experiments conducted at 9 m/s, the base of the wall actually ignited due to the accumulation of firebrands. These experiments demonstrate that it was very easy to produce ignition outside the structure since many firebrands were observed to accumulate in front of the structure during the tests. Although some firebrands were observed to enter the vents, the ignition of the wall assembly itself demonstrates the dangers of wind driven firebrand showers and that if only firebrand resistant vents are used, other vulnerabilities around a structure must be considered. It must be noted that the base of the wall assembly ignited without the presence of other combustibles that may be found near real structures (*e.g.* mulch, vegetation). As discussed above, the presence of combustibles placed near the test wall only made ignition easier.

7. Glazing assembly vulnerability

For some time, is has also been believed that firebrands become trapped, accumulate inside the corner of the framing of glazing assemblies, and may lead to window breakage. To investigate this potential vulnerability, two types of glazing assemblies were used for the experiments [33]. The first type was a horizontally sliding window assembly. The second type was a vertically sliding window assembly. Both of these glazing assemblies were double hung, since it is also thought that this type of assembly could provide more locations for firebrands to accumulate.

The sizes of each of the glazing assemblies were the same: 91 cm by 91 cm. To mount these assemblies, a 244 cm by 244 cm wall fitted with an open eave was constructed for testing. The wall was constructed using wood framing members spaced 406 mm (16'') on center. OSB was applied over the wood framing members and a moisture barrier was installed over the OSB. Vinyl siding was applied over the moisture barrier. An eave with a total length of 122 cm was constructed and mounted to the wall assembly. For completeness, an image of a typical experiment is shown in Fig. 18.

For, each window assembly considered, two different wind speeds were used. Specifically, the window assemblies were exposed to firebrand showers at wind tunnel speeds of 7 m/s and 9 m/s. At 7 m/s, a majority of the firebrands produced from the NIST Dragon were observed to be carried with the flow and impinge of the wall assembly. It was observed that firebrands accumulated within the framing and this behavior was more pronounced for the vertically sliding glazing assembly; as suspected. Yet, in none of the experiments did the framing sustain sufficient damage for the window assembly to cause glass fallout and/or breakage.

Please cite this article as: S.L. Manzello, et al., Enabling the study of structure vulnerabilities to ignition from wind driven firebrand showers: A summary of experimental results, Fire Safety J (2012), http://dx.doi.org/10.1016/j.firesaf.2012.06.012

Fig. 18. Picture of wall/eave assembly fitted with a vertically sliding, double hung window exposed to firebrand showers at a wind tunnel speed of 9 m/s [33]. The dimension of wall assembly was 244 cm by 244 cm.

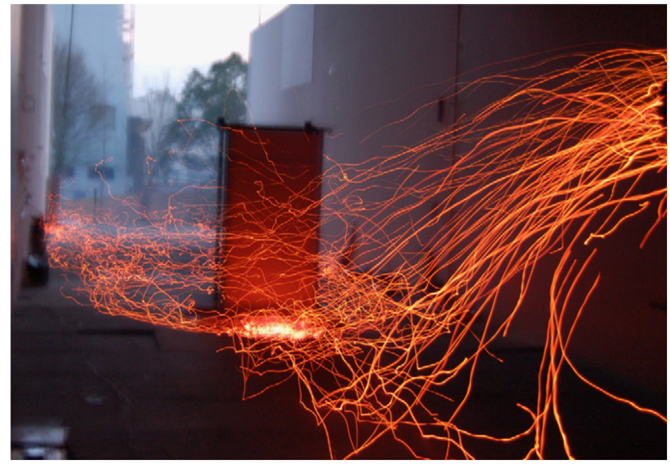

Fig. 19. Photograph taken by increasing the exposure time on the camera to visualize the firebrand streaklines or flow over the obstacles [23]. In this image, the obstacle dimensions were 2.0 m high by 1.0 m wide. The distance from the NIST Dragon to obstacle was 7.5 m.

8. Firebrand accumulation in front of obstacles

In these experiments, an obstacle was placed downstream of the firebrand showers inside the FRWTF. The same obstacle was oriented differently to have a different aspect ratio and thus allow for qualitative comparison of firebrand flow and the resulting stagnation plane where firebrands could potentially accumulate. When oriented lower to the ground, the obstacle dimensions were 1.0 m high and 2.0 m wide; for a higher orientation, the obstacle dimensions were 2.0 m high and 1.0 m wide. The front face of the obstacle was constructed from calcium silicate board. The distance of the NIST Dragon from the obstacles was the same as the structure experiments, namely 7.5 m downstream. In front of the obstacles, a series of wood boards (thickness of 9 mm) were placed flat on the ground of the FRWTF to determine if the accumulated firebrands were able to produce ignition events. The wood boards were not oven dried (moisture content 11% dry basis; see Eq. (1) for definition) in order to provide a greater barrier to produce ignition in these materials. A total of six experiments were conducted with three replicate tests for each obstacle orientation.

The presence of the obstacle resulted in a stagnation plane where numerous firebrands were able to accumulate. After the firebrands were observed to accumulate, intense glowing combustion was observed and in all cases, the accumulated firebrands produced an ignition event (SI) in the wood samples. A series of photographs was also taken by increasing the exposure time on the camera to visualize the firebrand flow process over the obstacles. This image is shown in Fig. 19.

9. Bench scale experiments—NIST dragon's lair facility

As demonstrated above, full-scale experiments are required to observe the vulnerabilities of structures to firebrand showers, but reduced-scale test methods afford the capability to evaluate firebrand resistant building elements and may serve as the basis for new standard testing methodologies. To this end, Manzello et al. [23] developed the NIST Dragon's Lofting and Ignition Research (LAIR) facility to simulate wind driven firebrand showers at reduced-scale. This facility consists of a reduced-scale Firebrand Generator (known as the NIST Baby Dragon) coupled to a bench-scale wind tunnel. The reduced-scale Dragon's LAIR facility was able to reproduce the results obtained from the full-scale experiments conducted pertaining to firebrand penetration through building vents described above [23].

While the NIST Dragon's LAIR facility and the full-scale NIST Dragon coupled to BRI's FRWTF have been used to expose building elements to firebrand showers, the duration of exposure using the existing apparatus is limited. To develop test methods needed to evaluate different building materials resistance to firebrand showers requires the capability to generate firebrand showers of varying duration.

Accordingly, the NIST reduced-scale continuous feed Firebrand Generator (the NIST continuous feed Baby Dragon) was developed. The unique features of the NIST continuous feed Baby Dragon, over the present NIST Dragon, are the ability to produce a constant firebrand shower in order to expose building materials to continual firebrand bombardment. In a very recent study, Suzuki and Manzello [39] characterized the performance of this device. Specifically, the number flux and mass flux were measured as a function of feeding rate to determine optimum conditions to generate steady firebrand showers. Another key issue is that the firebrand size and mass produced using the NIST continuous feed Baby Dragon has been tied to those measured from full-scale tree burns and actual WUI fires; similar to the NIST Dragon.

Recently, an effort was undertaken to construct a new and improved Dragon's LAIR facility. This entailed removing the NIST Baby Dragon from the wind tunnel facility and inserting the new and improved NIST continuous feed Baby Dragon. Further details are provided elsewhere [40].

Fig. 20 is a schematic of the new and improved NIST Dragon's Lofting and Ignition Research (LAIR) facility. The Dragon's LAIR consisted of a reduced scale continuous feed Firebrand Generator (Baby Dragon) coupled to a reduced scale wind tunnel. This version of the NIST reduced scale continuous feed Baby Dragon consisted of two parts; the main body and continuous feeding component. The feeding part was connected to the main body and had two gates to prevent fire spread. Each gate was opened and closed alternatively. A blower was connected to the main body.

A conveyer was used to feed wood pieces continuously into the device. The conveyer belt was set at 1.0 cm/s, and groups of wood pieces were put on the conveyer belt at 12.5 cm intervals. In each experiment, the group size placed on the conveyer belt was varied to allow for different firebrand exposures to the target (described below). For all tests, Douglas-fir wood pieces machined

Please cite this article as: S.L. Manzello, et al., Enabling the study of structure vulnerabilities to ignition from wind driven firebrand showers: A summary of experimental results, Fire Safety J (2012), http://dx.doi.org/10.1016/j.firesaf.2012.06.012

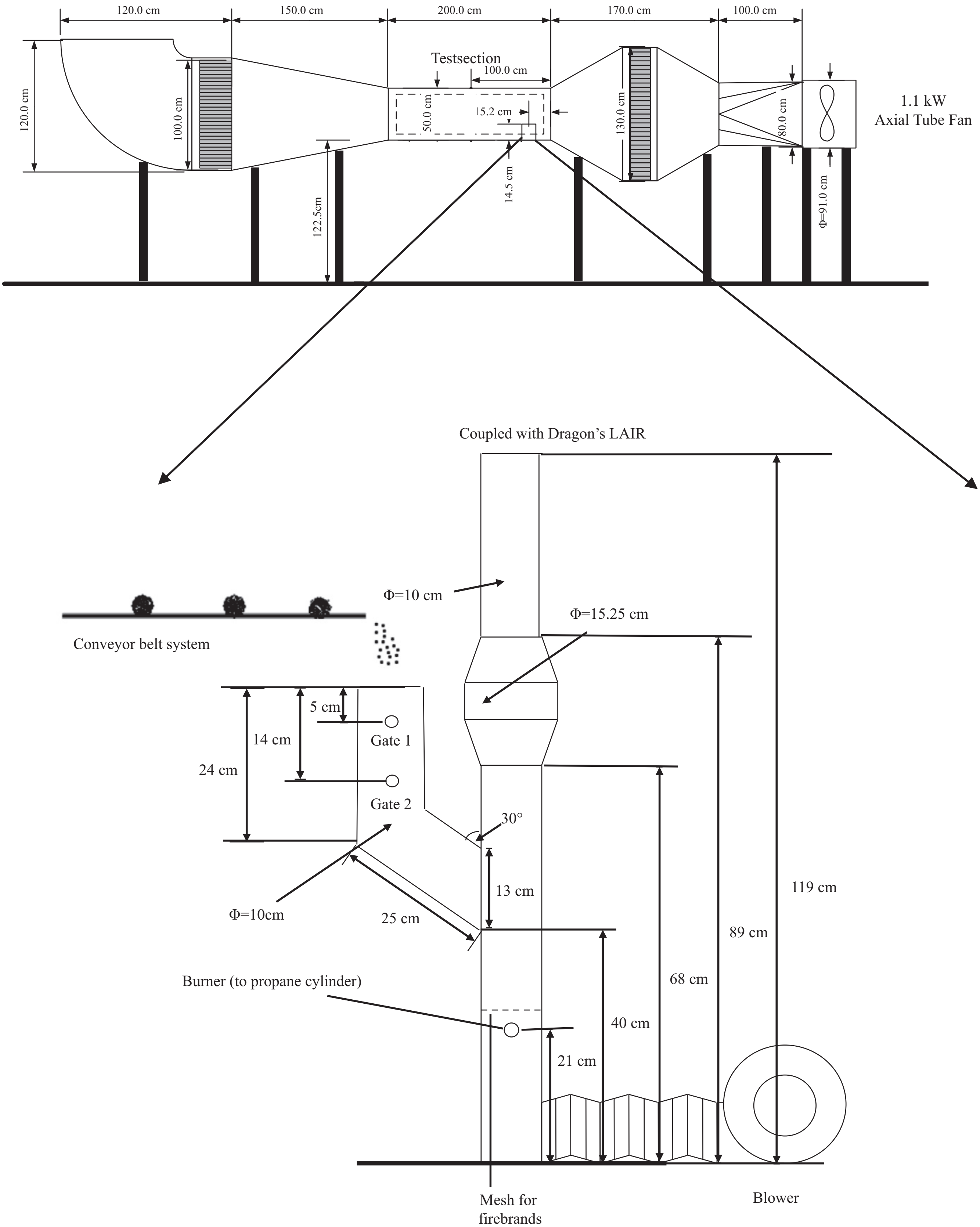

Fig. 20. Schematic of the new and improved NIST Dragon's Lofting and Ignition Research (LAIR) facility [40]. The Dragon's LAIR consisted of a reduced scale continuous feed Firebrand Generator (Baby Dragon) coupled to a reduced scale wind tunnel.

with dimensions of 7.9 mm (*H*) by 7.9 mm (*W*) by 12.7 mm (*L*) were used to produce firebrands. The reasons for using wood pieces for these experiments are provided elsewhere [23].

The test section of the wind tunnel was 50 cm × 50 cm × 200 cm. The flow was provided by an axial fan 91 cm in diameter. Hot wire anemometers were used to quantify the flow distribution and a calibration was determined as a function of wind tunnel fan frequency.

The efficacy of the new experimental facility to determine ignition regime maps of building materials exposed to continuous wind driven firebrand showers has been determined. To do this, cedar crevices were constructed for ignition testing. Two pieces of cedar were aligned at an angle of 60 degrees. This angle was selected since consistent ignition behavior has been observed for other building materials ignited by firebrands using this configuration [21,41]. The dimensions of each cedar piece used were 114 mm wide by 448 mm long. These dimensions were selected since the length covered nearly the entire wind tunnel length and the low width allowed for less flow obstruction. Since the cedar used in these experiments is used for siding, each piece was tapered. Specifically, the largest edge thickness was 11 mm and tapered down to 3 mm. Due to the arrangement of the crevice, the thick edge of each cedar piece was offset and this allowed for a nominal thickness of 7 mm at the center of the crevice where ignition (described below) was observed. The cedar pieces were held in place using a custom mounting bracket. The location of the cedar crevice was placed about 760 mm from the exit of the mouth of the NIST continuous feed Baby Dragon. This location was selected simply due to the fact that the firebrands were observed to land within the crevice using the wind speed selected in these experiments (6 m/s). The moisture content of the cedar pieces was varied using an oven. Specifically, experiments were conducted using cedar held at 11% moisture content (dry basis) as well as oven dried (placed within the oven held at 104 °C for four hours). Cedar was selected since it is a common material used for both siding and roofing assemblies.

The experiments were conducted in the following manner. The cedar crevice was placed inside the test section and the door of the test section was then closed. The blower of the NIST reduced scale continuous feed Baby Dragon was set at 4.4 m/s (to generate glowing firebrands) and one propane burner was ignited and inserted into the side of the device. The propane burner was kept on during the entire experiment. The conveyer was then switched on and wood pieces were fed into the stainless-steel pipe first, and then the gate near the conveyer was opened. The gate near the conveyer was then closed, and the other gate was then opened to allow the wood pieces to fall into the Dragon for ignition. Feeding continued for various durations; 5 min, 10 min, until ignition was observed. The experiments were recorded using a digital video recorder (30 frames per second) for subsequent analysis (described below).

Five different loadings of wood pieces were used for the ignition studies; 5, 10 15, 30, and 40 pieces. The mean mass for each loading was: 2.4 g for 5 pieces (feed rate of 11.7 g/min), 4.8 g for 10 pieces (feed rate of 23.1 g/min), 7.2 g for 15 pieces (feed rate of 34.6 g/min), 14.4 g for 30 pieces (feed rate of 69.1 g/min), and 19.1 g for 40 pieces (feed rate of 91.7 g/min), respectively. The uncertainty in the mass was 10%.

The number flux, at the exit of the device, was measured as a function of the feed rate. Mass flux data were calculated by multiplying the number flux and the average mass of each firebrand at different feed rates. To measure the firebrand mass, a series of water pans were placed downstream of the NIST Reduced Scale Continuous Feed Baby Dragon after firebrand production reached steady conditions. Water pans were used to quench combustion of the firebrands. If the water pans were not used, the firebrands would continue to burn and by the time collection was completed only ash would remain. These analyses

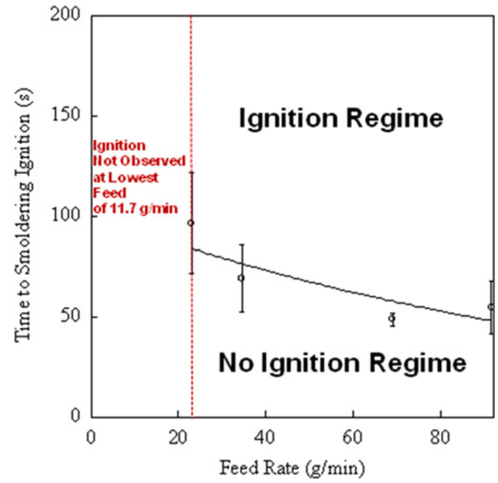

Fig. 21. Ignition regime maps (smoldering ignition) as a function of feed rate for fixed wind glowing firebrand generation rate for fixed wind tunnel speed (6 m/s) when using dried cedar crevices [40].

were critical to determine the mass generation rate of firebrands for each feed rate.

Ignition regime maps were determined as a function of feed rate (related to firebrand generation rate) for fixed wind tunnel speed (6 m/s) and two different cedar crevice moisture contents. Results are shown in Fig. 21. Ignition delay times were measured from the time the first firebrand was deposited inside the crevice to the observation of smoldering ignition (smoldering ignition, defined as intense glowing combustion within the cedar). Three repeat experiments were performed for each feed rate. Each data point represents the average of three experiments (average ± standard deviation). As can be seen, for a given moisture content and wind speed, the ignition delay time was observed to decrease as the feed rate was increased. This work has set the stage to be able to evaluate and compare the resistance to ignition from firebrand showers for the first time.

10. General remarks, future research, and summary

In this paper, a summary has been provided on an extended research effort to quantify structure vulnerabilities to wind driven firebrand showers. These results have laid the foundation for this important research direction. Nevertheless, it is important to discuss the findings in the context of actual WUI fires and consider paths for future research.

In real WUI fires, firebrand showers have been observed for several hours and with winds in excess of 20 m/s [42]. It was not possible to conduct experiments using higher wind speeds since the FRWTF was not designed to generate a wind field in excess of 10 m/s. Additionally, this version of the NIST Dragon was not designed to generate continuous firebrand showers so it was not possible to increase the duration of the firebrand exposure. Future work will consider:

- longer firebrand exposures,
- different firebrand size/mass distributions from Firebrand Generator,
- additional building components (e.g. boxed in eaves, other siding),
    - consider all of the above at higher wind speeds.

Progress is being made on all of these fronts. To address longer firebrand exposures, a new, full scale continuous feed Firebrand

Generator has been constructed and the basic premise of the device is a scaled up version of the continuous feed Firebrand Generator (Baby Dragon). The new full scale device has similar dimensions to the NIST Dragon (Fig. 1) presented here but allows for the production of continuous firebrand showers. In fact, experiments are now underway to determine the vulnerabilities of decking assemblies to wind driven firebrand showers using this newly developed experimental device. A workshop was held recently to provide input to these decking assembly experiments [43].

For the Firebrand Generator to generate different firebrand size/mass distributions, work is also in progress to determine firebrand production (size/mass) from building components and full scale burning structures [44,45]. Specifically, experiments have been conducted to determine firebrand production from actual building components/full scale burning structures since it is believed that structures themselves may be a significant source of firebrands, in addition to the vegetation. A figure of a full scale reentrant corner, ignited using a propane burner, and burning under an applied wind speed of 8 m/s is shown in Fig. 22 [45]. The influence of wind speed was considered by varying over a broad range; 8 m/s is shown. Firebrand size/mass distributions obtained from these experiments will be compared to those from burning vegetation and actual WUI fires.

To be able to consider higher wind speeds, NIST will partner with Insurance Institute for Business and Home Safety (IBHS). Specifically, IBHS has used the NIST Dragon concept to generate firebrand showers in their new (opened in 2011) full scale wind tunnel facility that is capable of wind speeds higher than 10 m/s [46]. At present, they have no capability to conduct continuous firebrand showers since they have implemented an array of firebrand generators based on the original NIST Dragon described in this paper. Now that NIST has developed the new, full scale continuous feed Firebrand Generator, it is expected that NIST will work with IBHS to implement this improved capability in their wind tunnel.

Fig. 22. Firebrand generation from a burning reentrant corner at 8 m/s applied wind [45]. Firebrands are produced on the backside of the assembly and are collected using an array of water pans downstream. The dimensions of each side of the reentrant corner were 122 cm by 244 cm.

Finally, the bench scale NIST Dragon's LAIR facility is a powerful tool with the capability to test new firebrand resistant technologies and serve as the basis for new standard testing methodologies. Reduced scale experiments allow many different types of firebrand resistant technologies to be tested and the performance of these technologies can then be verified using full scale testing. This experimental facility has also been reproduced by ADAI at the University of Coimbra in Portugal, Europe's largest research group focused on WUI fires.

Acknowledgments

Mr. Yu Yamamoto and Mr. Takefumi Yoneki of the Tokyo Fire Department (Guest Researchers at BRI) are acknowledged for their support of these experiments during SLM's stay in Japan in 2008. Dr. William 'Ruddy' Mell, Mr. Alexander Maranghides, Dr. Suel-Hyun Park, Mr. John R. Shields, and Dr. Jiann C. Yang of NIST are acknowledged for many helpful discussions during the course of the work. The Science and Technology Directorate of the U.S. Department of Homeland Security sponsored the production of this material under Interagency Agreement IAA HSHQDC-10-X-00288 with the National Institute of Standards and Technology (NIST).

References

[1] J.W. Mitchell, O.Patashnik, Firebrand protection as the key design element for structural survival during catastrophic wildfire fires, in: Proceedings of Fire and Materials 2007 Conference, San Francisco, CA, 2007.
[2] R. Blanchi, J.E. Leonard, R.H. Leicester, Lessons learnt from post-fire surveys at the urban interface in Australia, in: Proceedings of the Fifth International Conference on Forest Fire Research, Figueria da Foz, Portugal, 2006.
[3] A. Maranghides, W.E. Mell, A case study of a community affected by the Witch and Guejito fires, Fire Technol. 47 (2011) 379–420.
[4] F. Albini, Transport of firebrands by line thermals, Combust. Sci. Technol. 32 (1983) 277–288.
[5] A.Muraszew, J.F. Fedele, Statistical model for spot fire spread, The Aerospace Corporation Report no. ATR-77758801, Los Angeles, CA, 1976.
[6] C.S. Tarifa, P.P. del Notario, F.G., Moreno, On the Flight Paths and Lifetimes of Burning Particles of Wood Proceedings of the Combustion Institute 10, 1965, pp. 1021–1037.
[7] F. Albini, Spot fire distances from burning trees—a predictive model. USDA Forest Service General Technical Report INT-56, Missoula, MT, 1979.
[8] C.S. Tarifa, P.P. del Notario, F.G. Moreno, Transport and combustion of fire brands. Instituto Nacional de Tecnica Aerospacial "Esteban Terradas", Final Report of Grants FG-SP 114 and FG-SP-146, vol. 2, Madrid, Spain, 1967.
[9] S.D. Tse, A.C. Fernandez-Pello, On the flight paths of metal particles and embers generated by power lines in high winds and their potential to initiate wildfires, Fire Saf. J. 30 (1998) 333–356.
[10] J.P. Woycheese, Brand Lofting and Propagation for Large-Scale Fires, Ph.D. Thesis, University of California, Berkeley, 2000.
[11] I.K. Knight, The design and construction of a vertical wind tunnel for the study of untethered firebrands in flight, Fire Technol. 37 (2001) 87–100.
[12] R. Anthenien, S.D. Tse, A.C. Fernandez-Pello, On the trajectories of embers initially elevated or lofted by small scale ground fire plumes in high winds, Fire Saf. J. 41 (2006) 349–363.
[13] K. Himoto, T. Tanaka, Transport of disk shaped firebrands in a turbulent boundary layer, in: D.T. Gottuk, B.Y. Lattimer (Eds.), Fire Safety Science—Proceedings of the Eigth International Symposium, vol. 8, 2005, pp. 433–444, http://dx.doi.org/10.3801/IAFSS.FSS.8-433.
[14] N. Sardoy, J.L. Consalvi, A. Kaiss, A.C. Fernandez-Pello, B. Porterie, Numerical study of ground-level distribution of firebrands generated by line-fires, Combust. Flame 154 (2008) 478–488.
[15] E. Koo, P.J. Pagni, D.R. Weise, J.P. Woycheese, Firebrands and spotting ignition in large-scale fires, Int. J. Wildland Fire 19 (2010) 818–843.

[16] P.F. Ellis, The Aerodynamic and Combustion Characteristics of Eucalypt Bank—A Firebrand Study, Australian National University, Canberra, 2000, Ph.D. Dissertation.

[17] A. Ganteaume, C. Lampin-Maillet, M. Guijarro, C. Hernando, M. Jappiot, T. Fonturbel, P. Perez-Gorostiaga, J.A. Vega, Spot fires: fuel bed flammability and capability of firebrands to ignite fuel beds, Int. J. Wildland Fire 18 (8) (2009) 951–969.

[18] T.E. Waterman, Experimental Study of Firebrand Generation, Project J6130, IIT Research Institute, Chicago, IL, 1969.

[19] R.M. Hadden, S. Scott, C. Lautenberger, A.C. Fernandez-Pello, Ignition of combustible fuel beds by hot particles: an experimental and theoretical study, Fire Technol. 47 (2011) 341–355.

[20] S.L. Manzello, J.R. Shields, J.C. Yang, Y. Hayashi, D. Nii, On the use of a firebrand generator to investigate the ignition of structures in WUI Fires, in: Proceedings of the 11th International Conference on Fire Science and Engineering (INTERLFAM), Interscience Communications, London, 2007, pp. 861–872.

[21] S.L. Manzello, J.R. Shields, Y. Hayashi, D. Nii, Investigating the vulnerabilities of structures to ignition from a firebrand attack, in: B. Karlsson (Ed.), Fire Safety Science—Proceedings of the Ninth International Symposium, vol. 9, 2008, pp. 143–154, http://dx.doi.org/10.3801/IAFSS.FSS.9-143.

[22] S.L. Manzello, Y. Hayashi, Y. Yoneki, Y. Yamamoto, Quantifying the vulnerabilities of ceramic tile roofing assemblies to ignition during a firebrand attack, Fire Saf. J. 45 (2010) 35–43.

[23] S.L. Manzello, S.H. Park, J.R. Shields, S. Suzuki, Y. Hayashi, Experimental investigation of structure vulnerabilities to firebrand showers, Fire Saf. J. 46 (2011) 568–578.

[24] S.L. Manzello, J.R. Shields, T.G. Cleary, A. Maranghides, W.E. Mell, J.C. Yang, Y. Hayashi, D. Nii, T. Kurita, On the development and characterization of a Firebrand Generator, Fire Saf. J. 43 (2008) 258–268.

[25] S.L. Manzello, A. Maranghides, W.E. Mell, Firebrand generation from burning vegetation, Int. J. Wildland Fire 16 (2007) 458–462.

[26] S.L. Manzello, A. Maranghides, J.R. Shields, W.E. Mell, Y. Hayashi, D. Nii, Mass and size distribution of firebrands generated from burning Korean pine (*Pinus koraiensis*) trees, Fire Mater. J. 33 (2009) 21–31.

[27] E.I.D. Foote, J. Liu, S.L. Manzello, Characterizing firebrand exposure during wildland urban interface fires, in: Proceedings of Fire and Materials 2011 Conference, Interscience Communications, London, 2011.

[28] Standard Test Methods for Fire Tests of Roof Coverings, ASTM E108, American Society for Testing and Materials, West Conshohocken, PA.

[29] California Building Code, Title 24, Part 2, Chapter 7A, 2007, 〈http://www.bsc.ca.gov/default.htm〉.

[30] California Building Code, Title 24, Part 2, Chapter 7A, 2010, 〈http://www.bsc.ca.gov/default.htm〉.

[31] Official minutes ASTM E05.14 External Fire Exposure, June 17, 2009, 〈http://www.astm.org〉.

[32] S.L. Manzello, S. Suzuki, Summary of Workshop on Research Needs for Full Scale Testing to Determine Vulnerabilities of Siding Treatments and Glazing Assemblies to Ignition by Firebrand Showers, NIST SP 1111, 2010.

[33] S.L. Manzello, S. Suzuki, Y. Hayashi, Exposing siding treatments, walls fitted with eaves, and glazing assemblies to firebrand showers, Fire Saf. J. 50 (2012) 25–34.

[34] Vinyl Siding Installation Manual, Vinyl Siding Institute, 2007.

[35] Exterior and Interior Wall Manual, Cedar Shake and Shingle Bureau, 2004.

[36] S.L. Manzello, T.G. Cleary, J.R. Shields, J.C. Yang, Ignition of mulch and grasses by firebrands in wildland—urban interface (WUI) fires, Int. J. Wildland Fire 15 (2006) 427–431.

[37] S.L. Quarles, Y. Valachovic, G. Nakamura, G. Nader, M.J. De Saux, Home Survival in Wild Fire Prone Areas: Building Materials and Design Considerations, ANR Publication, 8393, , 2010.

[38] K. McGrattan, R. McDermott, S. Hostikka, J. Floyd, Fire Dynamics Simulator (Version 5) User's Guide, NIST Special Publication, 2010 1019–6.

[39] S. Suzuki, S.L. Manzello, On the development and characterization of a reduced scale continuous feed Firebrand Generator, in: M. Spearpoint (Ed.), Fire Safety Science—Proceedings of the Tenth International Symposium, vol. 10, 2011, pp. 1437–1448, http://dx.doi.org/10.3801/IAFSS.FSS.10-1437 2011.

[40] S.L. Manzello, S. Suzuki, The New and Improved NIST Dragon's LAIR (Lofting and Ignition Research) Facility, Fire Mater. J., doi: 10.1002/fam.1123, in press.

[41] S.L. Manzello, S.H. Park, T.G. Cleary, Investigation on the ability of glowing firebrands deposited within crevices to ignite common building materials, Fire Saf. J. 44 (2009) 894–900.

[42] J.W. Mitchell, Power lines and catastrophic wildland fire in Southern California, in: Proceedings of the 11th International Conference on Fire and Materials, San Francisco, CA, 2009, pp. 225–238.

[43] S.L. Manzello, S. Suzuki, Summary of 2011 Workshop on Research Needs for Full Scale Testing to Determine Vulnerabilities of Decking Assemblies to Ignition by Firebrand Showers, NIST SP 1129, 2011.

[44] S. Suzuki, S.L. Manzello, M. Lage, G. Laing, Firebrand generation data obtained from a full scale structure burn, Int. J. Wildland Fire, in press.

[45] S. Suzuki, S.L. Manzello, Y. Hayashi, The size and mass distribution of firebrands collected from ignited building components exposed to wind, in: Proceedings of the Combustion Institute, in preparation.

[46] 〈http://www.disastersafety.org〉.

Please cite this article as: S.L. Manzello, et al., Enabling the study of structure vulnerabilities to ignition from wind driven firebrand showers: A summary of experimental results, Fire Safety J (2012), http://dx.doi.org/10.1016/j.firesaf.2012.06.012